Astron. Astrophys. 341, 385–398 (1999)

ASTRONOMY AND ASTROPHYSICS

Influence of the metallicity and of the irradiation on the structure of accretion disks around massive black holes

Suzy Collin[1,⋆] **and Jean-Marc Huré**[1,2]

[1] Observatoire de Paris, Section de Meudon, Place Janssen, F-92195 Meudon, France
[2] Université Paris 7 (Denis Diderot), 2 Place Jussieu, F-75251 Paris Cedex 05, France

Received 25 March 1998 / Accepted 20 October 1998

Abstract. We discuss the structure of the outer regions of accretion disks around massive black holes, up to about one parsec from the center. In the gravitationally stable region, we assume the standard α-prescription for the viscosity but we take into account self-gravitation. Beyond about 10^4 gravitational radii, self-gravitation is larger than central gravitation, and the disk becomes gravitationally unstable. We then assume that it is maintained in a state of marginal instability such that the Toomre parameter stays of the order of a few units, as proposed by Paczynski (1978). The specificity of this prescription is that the midplane density is imposed as a function of the radius and depends only on the central mass. We demonstrate that the gas metallicity is of fundamental importance for the disk structure by considering two extreme cases: a pure hydrogen-helium mixture (i.e. a primeval gas), and a gas with solar abundances. In particular, the gravitationally unstable regions are optically thin in the case of primeval abundances while they remain optically thick for solar abundances. A consequence is that the midplane temperature is almost constant in the case of primeval abundances, and the disk is "flaring". Irradiation of the disk by the central UV-X source should thus be taken into account. We study the influence of this irradiation on the structure of a flaring disk, as well as in several other cases, and we show that it does not modify strongly the radial profile. We compute the column density of the ionized and atomic layers due to the irradiation, and show that they are much smaller than the column density of the molecular layer. Both for the non irradiated and for the irradiated disk, and for the primeval and for the solar metallicity cases, we give analytical expressions for the scale height and the midplane temperature which can be helpful to approximate the radial profile of an accretion disk in the molecular region. When applied to the masing disk of NGC 4258, these expressions show that the irradiation flux becomes dominant between 0.1 and 1 pc, depending on the value of accretion rate.

Key words: accretion, accretion disks – instabilities – galaxies: active – galaxies: nuclei – galaxies: quasars: general

Send offprint requests to: Suzy Collin (Observatoire de Meudon)
⋆ Research associate at Institut d'Astrophysique, Paris

1. Introduction

It is widely admitted that accretion of matter onto black holes in quasars and Active Nuclei of Galaxies (AGN) is mediated through an accretion disk. Proofs of the presence of accretion disks in AGN are obtained in particular from the observation of a privileged direction (radio jets, cones of ionized matter). The spectral distribution of quasars and AGN with its blue bump and soft X-ray excess is typical of the emission of an accretion disk (e.g. Malkan and Sargent 1983, and many subsequent papers). It is also likely that accretion disks are formed in the growing phase of primeval black holes, since rotation certainly affects the collapse, and the viscous time for transporting angular momentum is longer than the cooling time (Loeb and Rasio 1993).

The structure and emission of the central regions of accretion disks in AGN have been very often treated in the geometrically thin disk approximation with the prescription for turbulent viscosity introduced by Shakura and Sunayev (1973) (the so called "α-disks"). It assumes that the size of the turbulent eddies is smaller than the thickness of the disk and the turbulence is subsonic. Moreover the disk is stationary, implying that the accretion rate does not change during the time it takes for the gas to reach the black hole. Since this time is very short compared to the growing time and to the life time of the black hole, the stationary assumption is probably roughly valid at least for black holes lying in the strong gravitational potential of a protogalaxy and a rich gazeous environment. The α-prescription has proven to give satisfying results when applied to disks in cataclysmic variables and a relatively small value (≤ 0.1) of the α-parameter is generally invoked.

Compared to the innermost regions of the disk, the outer regions have been less investigated. At large radii, the self-gravity of the disk becomes larger than the vertical central gravity and must be taken into account. Such a study was performed, for instance by Huré et al. (1994a) with the Shakura and Sunayev's viscosity prescription. The authors stressed in particular the importance of using correct molecular and atomic opacities, and self-consistent disk equations including self-gravity. Self-gravity modifies strongly the structure of the disk with respect to the standard α-solution when it is of the order of the cen-

tral gravity. It is possible to find solutions of the disk structure even at large distances from the black hole, the density increasing rapidly with the radius and the disk scale height decreasing rapidly, but such solutions are not compatible with a steady state picture since they are gravitationally unstable, whatever the accretion rate (Huré 1998).

The α-prescription is probably no more valid in the gravitationally unstable region. Lin and Pringle (1987) proposed a prescription allowing for strongly unstable disks. They argued that in a self-gravitating disk, the largest size of the turbulent eddies stabilized by rotation, is Q times the disk thickness (Q being the Toomre parameter, see below). This prescription corresponds to a large (supersonic) viscosity. Shlosman, Frank and Begelman (1989) think that such a strongly self-gravitating thin disk would fragment, form stars, and be disrupted. On the contrary Paczyński (1978) proposed that a self-gravitating disk is maintained in a state of marginal instability (i.e. $Q =$ a few units), in which the energy dissipated by collisions between clumps prevent their collapse. A plausible picture, which is suggested by the observation of large molecular clouds in the Galaxy, is that a fraction of the disk stays gaseous and marginally unstable, and a fraction forms stars. We shall adopt this picture in the following paper where star formation and star evolution inside accretion disks and their subsequent influence on the metallicity are investigated (Collin & Zahn, 1998, and subsequent papers).

The present paper is devoted to the study of the structure of marginally unstable accretion disks. In Sect. 2 the structure of the disk is determined in the absence of an external radiation field, and the influence of the external irradiation on the vertical and radial structure is discussed in Sect. 3.

2. Structure of the non irradiated disk

An accretion disk becomes gravitationally unstable for non-axisymmetric perturbations when the parameter Q is smaller than a few units, Q being defined by:

$$Q = \frac{\Omega c_{\rm s}}{\pi G \Sigma}, \tag{1}$$

where Σ is the column density of the disk, $c_{\rm s}$ is the sound velocity and Ω is the Keplerian angular velocity (Toomre 1964, see also Goldreich and Lynden-Bell 1965). When Q is smaller than unity, the disk becomes also unstable for axisymmetric perturbations. As R increases, Q decreases monotonically in a α-disk (Huré 1998), and so the disk is unstable beyond a radius $R_{\rm T}$ (the "Toomre" radius) where $Q \sim 1$.

Outer regions of accretion disks are then divided in two parts: a gravitationally stable region ($R \leq R_{\rm T}$) where the α-prescription for the viscosity is used, and a gravitationally unstable region ($R \geq R_{\rm T}$) where the prescription for marginal instability is used instead (this expresses the fact that the viscosity is fine tuned so that the disk is marginally unstable). We shall see later that the results are not sensitive to the exact value defining the marginal unstability (see below).

For simplicity, we do not compute the vertical structure, and we adopt the picture of the vertically averaged disk where the physical quantities depend only on the radius. As shown for example by Canizzo & Reiff (1992) and Canizzo (1992), the radial profile is actually not very different when the vertical structure is taken into account. The basic equations are found in the appendix.

2.1. Equation of state and realistic opacities

The disk structure depends strongly on the opacity of the material, and therefore on the elementary species present in the gas and on their relative abundances with respect to hydrogen (Collin-Souffrin & Dumont, 1990, Huré et al. 1994b, Huré 1998). Since we want to apply our computations also to primeval gas, two different sets of chemical species are considered:

1. a gas with solar abundances (*i.e.*, $Z = Z_{\odot}$) including 72 chemical species, as described in Huré et al. (1994b): 11 neutral atoms: H, He, C, N, O, Ne, Mg, Si, S, Fe, Ti; 19 neutral molecules: H_2, CH, CH_2, CH_3, CH_4, O_2, OH, H_2O, CO, CO_2, HCO,NH, NH_2, NH_3, NO, CN, HCN, SiO, TiO; 15 ionized molecules: H_2^+, OH^+, H_3^+, O_2^+, CO^+, CH^+, CH_2^+, CH_3^+, CH_4^+, CH_5^+, H_2O^+, H_3O^+, HCO^+ HCO_2^+, CN^+; 5 negative ions: H^-, C^-, O^-, OH^-, CN^-; 11 single ionized atoms: H^+, He^+, C^+, N^+, O^+, Ne^+, Mg^+, Si^+, S^+, Fe^+, Ti^+; and 10 double ionized atoms: He^{++}, C^{++}, N^{++}, O^{++}, Ne^{++}, Mg^{++}, Si^{++}, S^{++}, Fe^{++}, Ti^{++}, and electrons;
2. a zero metallicity gas including hydrogen and helium only ($Z = 0$; 9 compounds plus electrons only remain).

We have computed numerically the ionisation and dissociation equilibria for the solar and the zero metallicity gas assuming LTE when it is justified. The Rosseland and Planck opacities $\kappa_{\rm R}$ and $\kappa_{\rm P}$ have been derived from frequency dependent absorption cross sections including molecular bound-bound absorption processes for CO, H_2O, TiO, CN, SiO, atomic bound-free and free-free transitions for hydrogen and helium, and electronic and Rayleigh diffusions due to H, H_2, He, C, N and O, also computed assuming LTE. Grain opacity is introduced smoothly below 2500 K but is not treated in detail. Actually we take a constant grain opacity of $1\,{\rm cm^2\,g^{-1}}$ below 1500 K, which is a reasonable approximation in the range 500-1500 K (Pollack et al. 1994).

Densities lower than $10^{12}\,{\rm cm^{-3}}$ are reached in the outermost regions and some chemical species depart from LTE. It is in particular the case of H^- which is an important coolant at temperatures near 5000 K (Huré 1994). Our results are therefore also approximate in this range.

In the zero metallicity case and below 2000 K, H_2 molecules are the main constituants of the gas and dominate the cooling. Provided that the temperature is larger than 500 K, the H_2 cooling function $\Lambda(T)$ can be computed assuming LTE, down to a density $10^7\,{\rm cm^{-3}}$ (i.e. Tine et al. 1997). At 500 K, even the lowest excited vibrational levels are underpopulated with respect to LTE if the ionization rate is small, and an underestimation of the cooling function follows. Above $10^8\,{\rm cm^{-3}}$, which is actually the smallest density reached in our computations, $\Lambda(T)$ depends little on the density (Lepp & Shull 1983, Smith & Mac

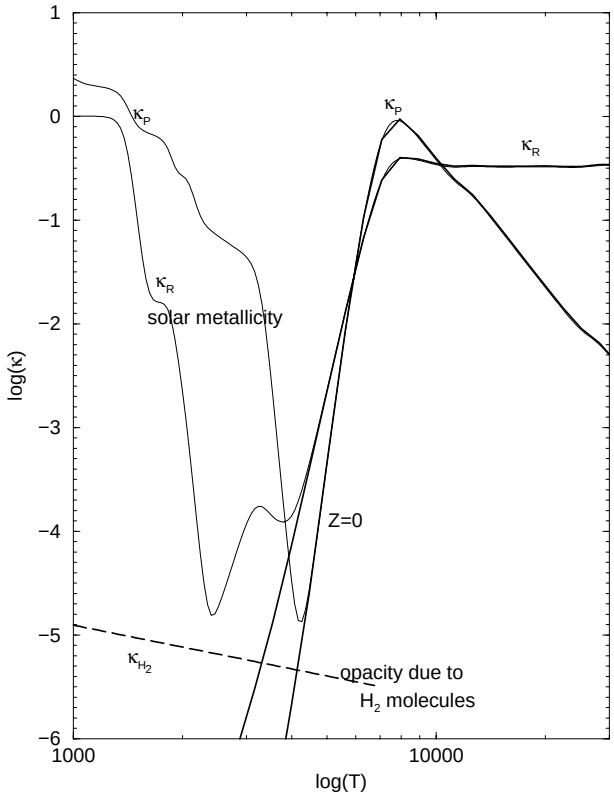

Fig. 1. The Rosseland mean opacity $\kappa_{\rm R}$ and the Planck mean opacity $\kappa_{\rm P}$, for a zero metallicity gas (bold lines) and for a solar metallicity gas (thin lines) as functions of the temperature, for $\rho = 10^{-12}\,{\rm g\,cm^{-3}}$, assuming LTE. Also plotted (bold dashed line) is the opacity due to H_2 molecules, computed according to the cooling function given by Smith & Mac Low (1997).

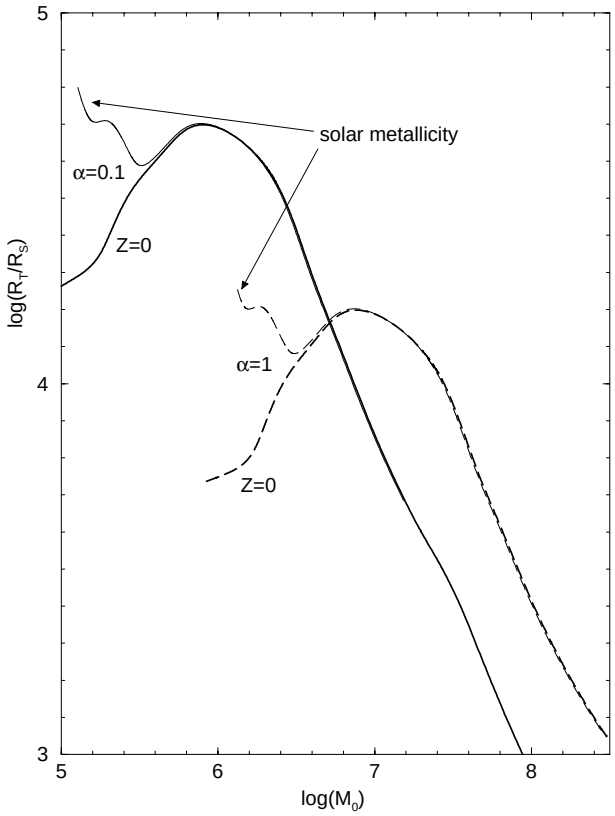

Fig. 2. The Toomre radius $R_{\rm T}$ (normalized to $R_{\rm S}$) versus the mass $\rm M_\odot$ of the black hole in units of $1\rm M_\odot$, computed for $Q = 2\sqrt{2}$, i.e. $\zeta = 1$. The accretion rate is critical. The α-parameter is labelled on the curves ($\alpha = 1$ is in dashed lines and $\alpha = 0.1$ is in solid lines). The zero metallicity case is plotted in bold lines and the solar metallicity case is in thin lines.

Low 1997). We therefore define an averaged absorption coefficient on the basis of the cooling function $\Lambda(T)$ for $Z = 0$ (see below, Eq. 14). Neither lithium nor deuterium have been taken into account, although it was recently noticed that HD cooling might dominate for temperatures smaller than 200 K (Puy 1997). Since the regions under study in this paper do not have such low temperatures, HD can be neglected.

For illustrative purpose the opacities are displayed in Fig. 1 for $Z = 0$ and $Z = Z_\odot$ and for $\rho = 10^{-12}\,{\rm g\,cm^{-3}}$. They vary within a large range. In particular, they are much smaller than unity for a primeval cold gas below a thousand degrees, while for metal enriched gas, they stay of the order of unity. As already noticed (Huré et al, 1994b, Alexander & Ferguson, 1994), the Rosseland mean opacity is smaller than the Planck opacity which is used in optically thin regimes (and the larger the density the larger the difference).

2.2. The onset of the gravitational instability

Given the opacity functions, we have computed the solutions of the α-disk equations (see Appendix Sect. A). We then have determined the Toomre radius, which is a function of the accretion rate and of α. For a given accretion rate normalized to the critical rate $\dot{m}_{\rm crit}$, $R_{\rm T}$ can be expressed as a function of M (here, we set $\dot{m}_{\rm crit} = L_{\rm Edd}/\eta c^2$, where $L_{\rm Edd}$ is the Eddington luminosity and η the mass energy conversion efficiency, taken equal to 0.1).

Fig. 2 displays the Toomre radius expressed in Schwarzschild radius $R_{\rm S} = 2GM/c^2 = 3\,10^5 M/\rm M_\odot$ cm as a function of the black hole mass in $\rm M_\odot$ for the critical accretion rate, for α = 0.1 and α = 1, and for the two metallicities. $R_{\rm T}$ is computed for $Q = 2\sqrt{2}$ (i.e. $\zeta = 1$, according to Eq. 4). We see that the Toomre radius expressed in $R_{\rm S}$ globally decreases with increasing mass. However, it stays of the order of 10^3 to a few 10^4 $R_{\rm S}$, which is comparable to the size of the Broad Line Region (may be it is not a coincidence!). These results are in good agreement with analytical expressions derived assuming constant opacity coefficient and mean mass per particle μ. Actually, for $M_6 \lesssim 20\,\alpha^{2/5}$ (self-gravition plays a role inside the gas pressure dominated regions only, see Huré 1998), one finds:

$$\frac{R_{\rm T}}{R_{\rm S}} \simeq 5.5\times 10^4 \alpha^{14/27}\mu^{-8/9}\kappa_{\rm R}^{2/9} f_{\rm E}^{-8/27} M_6^{-26/27}, \qquad (2)$$

while for higher central masses, one gets:

$$\frac{R_{\rm T}}{R_{\rm S}} \simeq 4.2\times 10^4 \alpha^{2/9}\kappa_{\rm R}^{2/3} f_{\rm E}^{4/9} M_6^{-2/9}, \qquad (3)$$

where M_6 is the black hole mass expressed in units of $10^6 \mathrm{M}_\odot$, and f_E is the ratio of the bolometric to the Eddington luminosity (or the ratio of the accretion rate to the critical accretion rate, for a given mass energy conversion efficiency). For quasars, $0.1 \leq f_\mathrm{E} \leq 1$. In both cases, the sensitivity to the α-parameter and specially to the opacity are strong, meaning that it is worthwhile to perform self-consistent calculations including realistic opacities and equation of state.

In the following, we shall use $\alpha = 0.1$ for computing the disk structure in the gravitationally stable region.

2.3. The marginally unstable region

Let us now study the regions located beyond the Toomre radius, according to the marginal instability prescription. Optically thick and thin cases have been considered.

Our detailed computations revealed that, for any black hole mass, beyond the Toomre radius:

- the disk is **optically thick** for **a solar metallicity** gas.
- the disk is **optically thin** for a **zero metallicity** gas.

We shall discuss these two cases separately. Mainly to enlighten the upcoming discussion, we derive first analytical solutions assuming constant opacity coefficients. The mean molecular mass μ is also set equal to unity (while it varies between 0.6 and 2.4). We introduce the parameter:

$$\zeta = 4\pi G\rho/\Omega^2 \tag{4}$$

where ρ is the density at the equatorial plane. Thus $Q = 2\sqrt{1+\zeta}/\zeta$.

2.3.1. Solar metallicity, optically thick disk

When the gas pressure dominates on the radiative one, the equations given in the appendix provide the following solutions in the limit of great optical depths:

$$\rho \;=\; 5.9\times10^{-9}\;\zeta\;M_6^{-2}\;R_4^{-3} \qquad \mathrm{g\;cm^{-3}} \tag{5}$$

$$T \;=\; 3\times10^{4}\;\frac{\zeta^{2/7}}{(1+\zeta)^{1/7}} f_\mathrm{E}^{2/7}\;M_6^{-4/7}\;R_4^{-9/7}\kappa_\mathrm{R}^{2/7}\;\;\mathrm{K} \tag{6}$$

$$H \;=\; 2.2\times10^{13}\frac{\zeta^{1/7}}{(1+\zeta)^{4/7}} f_\mathrm{E}^{1/7}\;M_6^{5/7}\;R_4^{6/7}\kappa_\mathrm{R}^{1/7}\;\;\mathrm{cm} \tag{7}$$

where H is the scale height of the disk (about its half thickness), and T is the midplane temperature. In these relations $\zeta = 4.83$ when $Q = 1$. We choose as a reference radius $R_4 = 10^4 R_\mathrm{S}$, because it is of the order of the Toomre radius.

From Eqs. 5 and 7, one can easily deduce the surface density $\Sigma = 2\rho H$:

$$\Sigma = 2.6\times10^{5}\frac{\zeta^{8/7}}{(1+\zeta)^{4/7}} f_\mathrm{E}^{1/7} M_6^{-9/7} R_4^{-15/7}\kappa_\mathrm{R}^{1/7}\;\mathrm{g\;cm^{-2}}, \tag{8}$$

which provides the Rosseland optical thickness $\tau_\mathrm{R} = \Sigma\kappa_\mathrm{R}/2$.

Finally, since the disk is marginally unstable, it can fragment into clouds whose mass M_frag is of the order of ρH^3 (Goldreich & Lynden-Bell, 1965). Eqs. 5 and 7 give then:

$$M_\mathrm{frag} \;\sim\; 3\times10^{-2}\zeta^{10/7}(1+\zeta)^{-12/7} \times f_\mathrm{E}^{3/7}\;M_6^{1/7}R_4^{-3/7}\kappa_\mathrm{R}^{3/7}\mathrm{M}_\odot. \tag{9}$$

Below 1500K κ_R is of the order of unity (see Fig. 1), and a few interesting results can be drawn from these expressions:

- the disk structure depends little on the Eddington ratio f_E, but depends quite strongly on the mass of the black hole, so we will have to discuss separately low mass and high mass black holes.
- the density and the column density drop very rapidly with the radius. This is due to the marginal instability prescription which imposes a decrease of the density to compensate the effect of the decrease of central gravity.
- the scale height increases less rapidly than the radius. This means that the disk does not "flare", and that the outer regions do not see the central UV and X-ray ionizing radiation, unless this central source has a special geometry. We shall discuss this possibility in the next section.
- the temperature decreases rapidly with increasing radius, and the gas in the outer regions is molecular.

2.3.2. Zero metallicity, optically thin disk

Since the variation of the density with the radius does not involve the energy equation, ρ is not modified with respect to the optically thick case, and Eq. 5 always applies. Assuming a constant opacity coefficient, the other quantities become:

$$T \;=\; 1.65\times10^{2}\frac{(1+\zeta)^{1/9}}{\zeta^{2/9}}\;f_\mathrm{E}^{2/9}\;R_4^{-1/3}\kappa_\mathrm{P}^{-2/9}\;\;\mathrm{K} \tag{10}$$

$$H \;=\; 1.7\times10^{12}\;\frac{(1+\zeta)^{4/9}}{\zeta^{1/9}}\;f_\mathrm{E}^{1/9}\;M_6\;R_4^{4/3}\kappa_\mathrm{P}^{-1/9}\;\;\mathrm{cm} \tag{11}$$

$$\Sigma \;=\; 2\times10^{4}\frac{\zeta^{8/9}}{(1+\zeta)^{4/9}} f_\mathrm{E}^{1/9} M_6^{-1} R_4^{-5/3}\kappa_\mathrm{P}^{1/9}\;\;\mathrm{g\;cm^{-2}}. \tag{12}$$

The Planck optical thickness follows from the latter equation.

In the molecular region, hydrogen molecules play a double role: they are the main gas component and they are the main source of emission. It is then possible to go a step further with analytical expressions for $T \leq 1800\,\mathrm{K}$, using a simplified function for the H_2 cooling $\Lambda(T)$ (Smith & Mac Low 1997):

$$\Lambda(T) = 4.2\times10^{-31}\;T^{3.3}\;\;\mathrm{erg\;s^{-1}}. \tag{13}$$

This cooling function can easily be converted into an opacity function $\kappa_{\mathrm{H2}}(T)$ which depends on the temperature only:

$$\kappa_{\mathrm{H2}}(T) = 4.4\times10^{-3}\;T^{-0.7}\;\;\mathrm{cm^2\;g^{-1}}. \tag{14}$$

It turns out that the temperature, the scale height, the surface density and the optical thickness, write respectively:

$$T \;=\; 2.2\times10^{3}\left(\frac{1+\zeta}{\zeta^2}\right)^{0.132}\;f_\mathrm{E}^{0.263}\;R_4^{-0.395} \qquad \mathrm{K} \tag{15}$$

$$H = 6.2\times10^{12}\,\zeta^{-0.132}(1+\zeta)^{-0.433} \times f_{\rm E}^{0.132}\,M_6\,R_4^{1.3}\ {\rm cm} \quad (16)$$

$$\Sigma = 7.3\times10^{4}\frac{\zeta^{0.866}}{(1+\zeta)^{0.433}}f_{\rm E}^{-0.132}M_6^{-1}R_4^{-1.7}\ {\rm g\,cm^{-2}} \quad (17)$$

$$\tau_{\rm P} = 0.67\,\zeta^{0.165}(1+\zeta)^{-0.081}\,f_{\rm E}^{-0.054}\,M_6^{-1}\,R_4^{-1.4}. \quad (18)$$

These equations show that the temperature and the optical thickness decrease with increasing radius, and the scale height increases more rapidly than the radius. Due to this flaring, we have to consider the effect of radiation of the central regions on the structure of outer regions (see Sect. 3).

Finally, one finds the mass of the fragments from Eqs. 5 and 16:

$$M_{\rm frag} \simeq 7\times10^{-4}\frac{\zeta^{0.604}}{(1+\zeta)^{1.30}}\,f_{\rm E}^{0.396}\,M_6\,R_4^{0.9}\ {\rm M_\odot}. \quad (19)$$

2.4. Disk structure with realistic opacities

We have solved the disk equations numerically by a method described in Huré (1998), including realistic opacities. The variation with the radius of the temperature, the density, the mean optical thickness, the ratio H/R, the surface density, and the mass of the fragments, are displayed in Figs. 3 and 4 for $M = 10^6$ $\rm M_\odot$ and $M = 10^8$ $\rm M_\odot$, with $f_{\rm Edd}$=1.

For comparison, the figures show also the results obtained with the analytical expressions using $\kappa_{\rm R} = 1\,{\rm cm^2\,g^{-1}}$, in the solar metallicity case. They confirm that the analytical laws give a valuable approximation of the real solutions (except for the masses of the fragments, which depend strongly on the scale height). In particular the location of the Toomre radius is given with an accuracy better than 40% by the analytical solution.

As already noticed in other studies, there is a range of radii where multiple solutions exist. These multiplicity might be due to the vertical averaging, and could disappear in a model with a vertical structure. If they are real, the choice between the different solutions would be determined by the past history of the inflowing gas, and a shock should settle near the radius of the discontinuity. Also we have not retained solutions at $R < R_{\rm T}$ found with the marginal instability criterium, which are probably non physical.

The temperature is low and the gas is molecular beyond the Toomre radius for $M_6 = 1$, i.e. at 0.003 pc. For $M_6 = 100$ the gas becomes molecular at a larger radius, ~ 0.03 pc for the solar metallicity and 0.3 pc for the zero metallicity. Comparing the zero and the solar metallicity cases shows that above 4000 K the temperature is the same, as hydrogen is the most efficient coolant, while below 4000 K, the temperature is smaller in the solar metallicity case, as cooling is dominated by heavy elements locked in molecules, and by dust for $T \leq 1500$ K.

The masses of the fragments vary between 0.1 and 10 $\rm M_\odot$ for M_6=100 for both zero and solar metallicity. For M_6=1 they are smaller, and they increase with R in the zero metallicity case, and decrease in the solar case.

3. Influence of an external irradiation

It is often mentioned that the outer regions of accretion disks are ionized and heated by the UV and X–ray photons produced in the inner regions, which inhibit star formation. Observations of AGN, in particular of their variability and of the spectral distribution in hard X-rays, indeed strongly suggest that an X–ray source lies at the center of the nucleus at about 10 $R_{\rm S}$ and illuminates the inner regions of the disk as well as the BLR. An external radiation field can have strong effects on the accretion disk: modifying the energy balance (and therefore the temperature and the scale height), changing the ionization rate (and therefore the chemical and statistical equilibrium of molecules).

The external radiative flux varies in general less rapidly with R than the viscous flux does (see below). There is thus a radius $R_{\rm crit}$ beyond which the external flux is larger than the viscous flux. It is generally believed that beyond this radius the vertical structure of the disk is modified with respect to the pure viscous case. This is not true if the disk has a large optical thickness, and the condition for radiative heating to dominate on viscous heating inside the disk when $\tau_{\rm R}$ is larger than unity (Huré et al. 1994a) is:

$$F_{\rm visc}\,(1+\frac{3}{8}\tau_{\rm R}) \leq \frac{F_{\rm inc}}{2} \quad (20)$$

where $F_{\rm inc}$ is the radiative flux incident on the disk, and $F_{\rm visc}$ is the viscous flux per face of the disk (right hand side of Eq. A5).

When the disk is optically thin (in the sense of the Planck mean), the midplane temperature is increased and the radial profile modified accordingly, if $F_{\rm inc}$ is larger than $F_{\rm visc}$. However one should remind that even in this case, if the surface density is large, the ionizing fraction of the flux is also absorbed in a thin layer, and only IR and visible photons on the one hand, and hard X–ray photons on the other hand, can penetrate inside the disk.

It is expected that the midplane temperature radial profile is very different in the optically thin and in the optically thick cases when the viscous flux is negligible. In the optically thick case, the midplane temperature is:

$$T \sim \left(\frac{F_{\rm inc}\tau_{\rm R}}{\sigma}\right)^{1/4}. \quad (21)$$

As $F_{\rm inc}$ decreases rapidly with the radius, T also decreases. While in the optically thin case, it is:

$$T \sim \left(\frac{F_{\rm inc}}{\sigma}\right)^{1/4}. \quad (22)$$

The optically thin (primeval) and the optical thick (solar) cases correspond therefore to quite different effects of the external radiation.

We shall first examine different possibilities for an external irradiation of the disk, then compute the radius at which it becomes dominant on the viscous flux in the midplane and give the corresponding radial profiles, finally verify that the vertical structure is not strongly modified and that the bulk of the outer disk remains molecular.

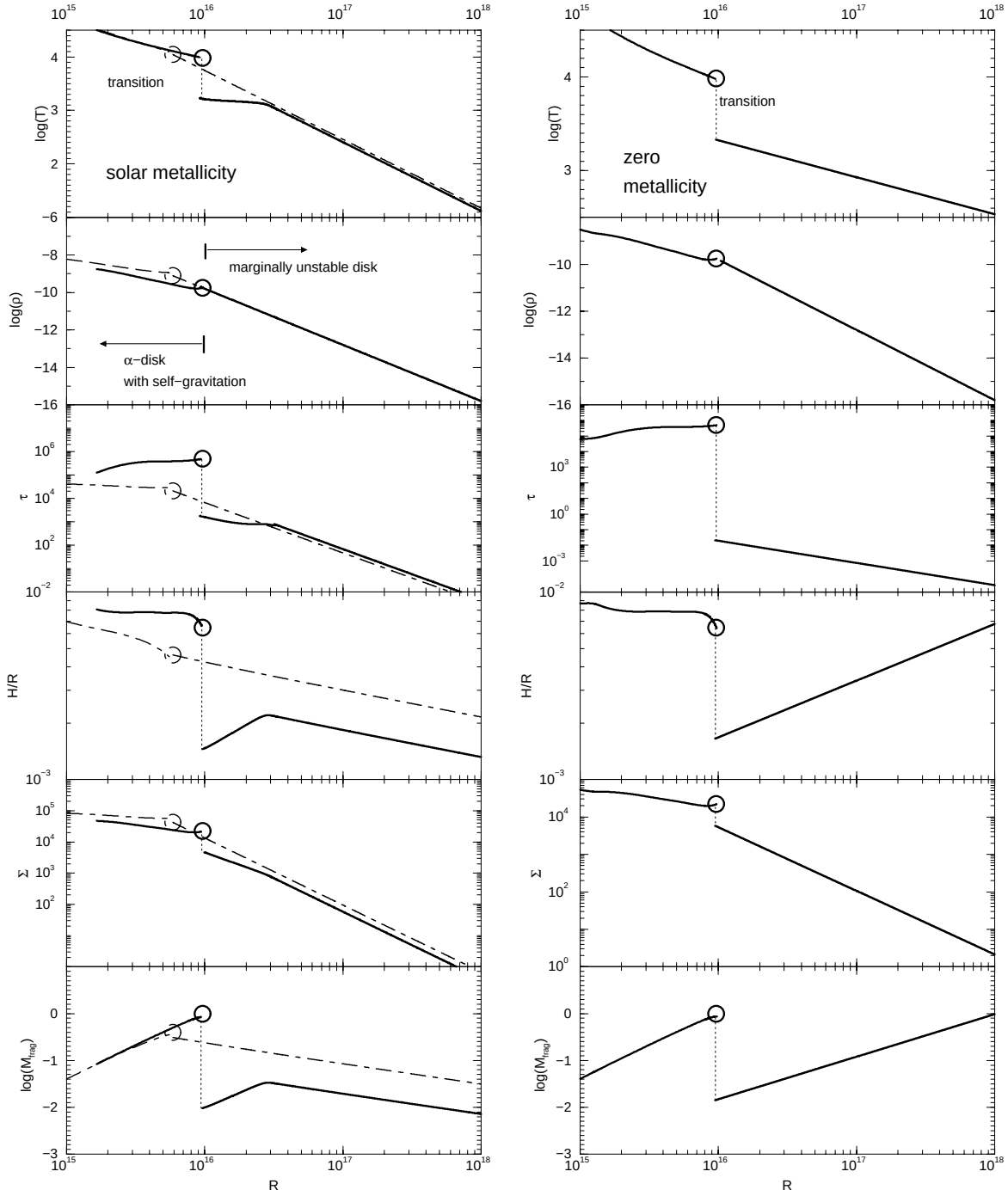

Fig. 3. From *top* to *bottom*: T, ρ, $\tau_{\rm R}$ or $\tau_{\rm P}$, H/R, Σ, and $M_{\rm frag}$ in $\mathrm{M}_\odot$, as functions of the radius in cm for $M_6 = 1$. The Toomre radius is indicated with a circle. It is computed for $Q = 2\sqrt{2}$ and the accretion rate is assumed critical. For $R \leq R_{\rm T}$ $\alpha = 0.1$. A possible disk solution is given in plain bold. *Left:* solar metallicity; *right:* zero metallicity. In the solar metallicity case the analytical expressions with $\kappa_{\rm R} = 1\,\mathrm{g}^{-1}\,\mathrm{cm}^2$ are shown in dot–and–dashed lines.

3.1. The external radiative flux

There are several ways for the outer regions of the disk to "see" a central source of radiation: either the source has a large spatial extension, or the disk flares or is warped, or finally the central radiation is backscattered by a hot medium. An example of warping is the "masing" disk of NGC 4258, where the disk is warped with an angle of about 10°. Backscattering is proposed as an explanation of the emission of broad lines by the surface of the disk (Dumont & Collin-Souffrin 1990). This is a potentially important way of illuminating the disk if the hot medium has a Thomson optical thickness close to unity and a large spatial extension.

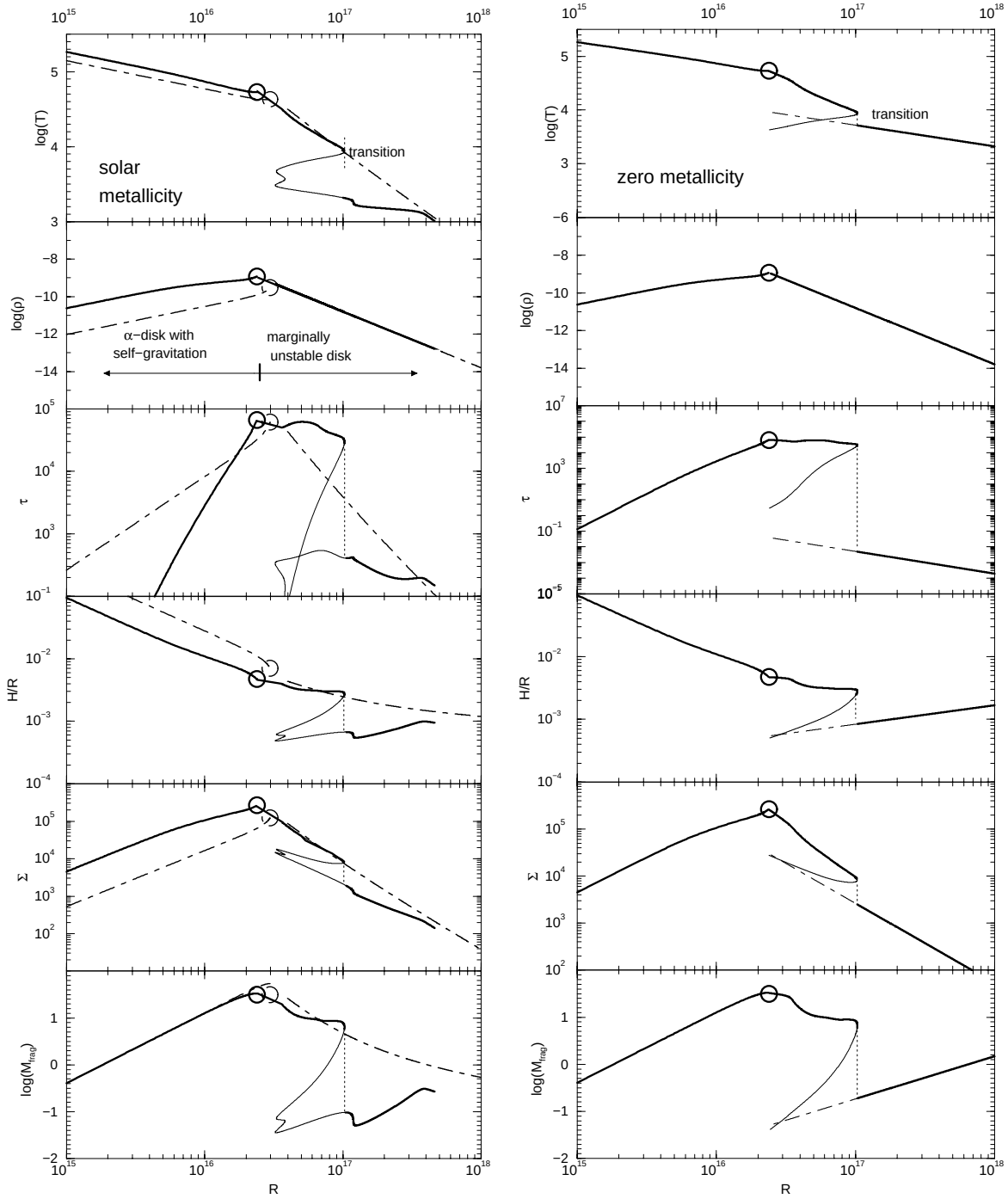

Fig. 4. Same legend as for Fig. 3 but for $M_6 = 100$.

3.1.1. The central source has a large spatial extension

In this case, the disk sees directly the central source which is for example a sphere with a radius A, or which consists of a point source located at a height A above the disk.

In the following we call $f_{\rm inc}$ the proportion of the bolometric luminosity heating the disk. It accounts for the radiation reflected by the disk, for the fraction of the Lyman continuum absorbed near the surface and not reprocessed towards the interior, and for a possible non isotropy of the ionizing source.

For a spherical source with no limb darkening, the incident flux on one face of the disk is (Hubeny 1990):

$$F_{\rm inc} = f_{\rm inc} \frac{L_{\rm bol}}{4\pi^2 A^2} \left[\theta' - \sin\theta' \cos\theta'\right], \quad (23)$$

where $L_{\rm bol}$ is the bolometric luminosity and θ' is given by $\sin\theta' = A/R$.

For a point source above the disk surface, $F_{\rm inc}$ writes:

$$F_{\rm inc} = f_{\rm inc} \frac{L_{\rm bol}}{8\pi(R^2 + A^2)} \sin\theta, \quad (24)$$

where θ is the incidence angle of the light rays on the disk surface.

X–ray variability studies suggest that A is of the order of $10R_{\rm S}$, while we are interested in regions located much further away. For $R \gg A$, these two expressions take a similar form:

$$F_{\rm inc} = f_{\rm inc}\frac{L_{\rm bol}}{4\pi R^2}\frac{A}{R}, \tag{25}$$

where $f_{\rm inc}$ is replaced by $f_{\rm inc}/2$ for the point source and by $2f_{\rm inc}/3\pi$ for the spherical source.

Actually in the last case the external radiative flux varies as R^{-3} like the viscous flux and is always smaller, so $R_{\rm crit}$ does not exist.

3.1.2. The disk flares or is warped

If the scale height is proportional to R^β, one can show that $F_{\rm inc}$ writes:

$$F_{\rm inc} = f_{\rm inc}\frac{L_{\rm bol}}{4\pi(R^2+H^2)^{3/2}}\frac{RH(\beta-1)}{(R^2+\beta^2H^2)^{1/2}}. \tag{26}$$

For a thin disk such that $H/R \ll 1$, this expression becomes simply:

$$F_{\rm inc} = f_{\rm inc}(\beta-1)\frac{L_{\rm bol}}{4\pi R^2}\frac{H}{R}. \tag{27}$$

If the disk is warped with an angle θ (which for simplicity we assume constant), $F_{\rm inc}$ is equal to:

$$F_{\rm inc} = \sin\theta\, f_{\rm inc}\frac{L_{\rm bol}}{4\pi R^2}. \tag{28}$$

3.1.3. The light emitted by the central source is backscattered towards the disk

We assume that there is a scattering medium with a density distribution $\propto R^{-m}$, with $1 \leq m \leq 2$ (a wind or a spherical stationary accretion flow corresponds to $m = \frac{3}{2}$). The flux backscattered towards the disk is then given by (Dumont & Collin-Souffrin 1990):

$$F_{\rm inc} \sim \tau_{\rm T}\, f_{\rm inc}\frac{L_{\rm bol}}{4\pi R^2}\left(\frac{R_{\rm X}}{R}\right)^g, \tag{29}$$

where $0 \leq g \leq 1$ ($g \sim 0.5$ for $m = \frac{3}{2}$), $\tau_{\rm T}$ is the Thomson optical thickness of the hot medium (necessarily smaller than unity), and $R_{\rm X}$ can be identified with the radius of the central source (i.e., $R_{\rm X} \approx A$).

In summary we have to consider three different functional forms of $F_{\rm inc}$ in order to take into account all possibilities:

– for indirect irradiation (with $g \sim 0.5$):

$$F_{\rm inc} = f\frac{L_{\rm bol}}{4\pi R^2}\left(\frac{R_{\rm X}}{R}\right)^g; \tag{30}$$

– for the warped disk:

$$F_{\rm inc} = f\frac{L_{\rm bol}}{4\pi R^2}; \tag{31}$$

– for the flaring disk:

$$F_{\rm inc} = f\frac{L_{\rm bol}}{4\pi R^2}\frac{H}{R}. \tag{32}$$

In these equations, f is typically at most of the order of 0.1, since it takes into account $f_{\rm inc}$ and other factors, some of them being possibly much smaller than unity, such as the cosine of the warping angle. One should also not forget that if the UV and soft X-ray continuum is emitted by the inner regions of the disk, it presents, as for any atmosphere, a limb darkening effect, and the intensity is more intense in the direction normal to the disk than at low incidence. It is not possible to know the exact dependence of the intensity with the direction, since it depends on the structure of the atmosphere, but if one assumes a simple $\cos\theta$ dependence, it means that f should be multiplied by an extra factor $\sin\theta$ or H/R in Eqs. 31 and 32. Purposely, we adopt $f_{-1} = f/0.1$ in order to get an overestimation of $F_{\rm inc}$ and of its influence on the disk structure.

3.2. Radial profile

As a first step, we assume that the external radiation is absorbed before reaching the midplane of the disk, and only reprocessed visible and infrared radiation penetrate in the deepest layers. Such radiation contributes only to the heating and does not produce any extra ionization.

3.2.1. Solar metallicity, optically thick disk

We have seen (Figs. 3 and 4) that in the case of solar abundances the disk is not flaring and is optically thick up to large radii. Therefore the only possibilities for irradiation are: backscattering of the central radiation (Eq. 30 with $g = 0.5$), and warping of the disk (Eq. 31).

According to Eq. 20 the external radiative flux dominates on the viscous flux when $F_{\rm visc}\tau_{\rm R} \lesssim F_{\rm inc}$. To compute $\tau_{\rm R}$ and then $R_{\rm crit}$, one can use the solutions given either by the irradiation or by the viscous dominated flux. We choose to perform the computation with the viscous dominated disk. Using then Eqs. 5, 8, and either Eq. 30 or Eq. 31, this condition gives:

$$\begin{aligned} R_{4,\rm crit} \;=\; & 67\frac{\zeta^{16/37}}{(1+\zeta)^{8/37}} f_{\rm E}^{2/37} f_{-1}^{-14/37} \\ & \times M_6^{-18/37} r_{\rm X,1}^{-7/37} \kappa_{\rm R}^{16/37}, \end{aligned} \tag{33}$$

for the backscattering case, and

$$R_{4,\rm crit} = 12\frac{\zeta^{8/22}}{(1+\zeta)^{4/22}} f_{\rm E}^{1/22} f_{-1}^{-7/22} M_6^{-9/22} \kappa_{\rm R}^{8/22}, \tag{34}$$

for the warped disk, where $r_{\rm X,1}$ is the radius of the X–ray source expressed in $10R_{\rm S}$.

It is interesting to note that **the results are almost independent of the Eddington ratio**. Eq. 34 shows that in the case of backscattering the external radiative flux does not change the radial profile up to a radius of the order of 10^{-1} parsec for $M = 10^6 M_\odot$ and 1 parsec for $M = 10^8 {\rm M}_\odot$. In the case of a

warped disk, $R_{\rm crit}$ becomes 10^{-2} parsec for $M = 10^6 {\rm M}_\odot$ and 10 parsec for $M = 10^8 {\rm M}_\odot$. So the external radiation can be important in the outer regions of the disk.

Using Eqs. 21 and A1, and either Eq. 30 or Eq. 31, one finds the pure irradiation solutions valid beyond the critical radius given by Eq. 33 (respt.34) in the backscattering case (respt. in the warped case).

For the backscattering case, one gets:

$$T = 2.8\times10^3 (f_{-1}f_{\rm E})^{1/4} r_{\rm X,1}^{1/8} M_6^{-1/4} R_4^{-5/8} {\rm K} \quad (35)$$

$$H = 6.9\times10^{12} \frac{1}{(1+\zeta)^{1/2}} (f_{-1}f_{\rm E})^{1/8} \times r_{\rm X,1}^{1/16} M_6^{7/8} R_4^{19/16} {\rm cm} \quad (36)$$

$$\Sigma = 8.1\times10^4 \frac{\zeta}{(1+\zeta)^{1/2}} (f_{-1}f_{\rm E})^{1/8} \times r_{\rm X,1}^{1/16} M_6^{-9/8} R_4^{-29/16} \ {\rm g\ cm^{-2}}. \quad (37)$$

For the warped disk, one gets:

$$T = 6.7\times10^3 (f_{-1}f_{\rm E})^{1/4} M_6^{-1/4} R_4^{-1/2} {\rm K} \quad (38)$$

$$H = 1.1\times10^{13} \frac{1}{(1+\zeta)^{1/2}} (f_{-1}f_{\rm E})^{1/8} M_6^{7/8} R_4^{5/4} {\rm cm} \quad (39)$$

$$\Sigma = 1.25\times10^4 \frac{\zeta}{(1+\zeta)^{1/2}} \times (f_{-1}f_{\rm E})^{1/8} M_6^{-9/8} R_4^{-7/4} {\rm g\ cm^{-2}}. \quad (40)$$

Several interesting results are worthy of note:

1. the solutions are very similar in both cases; in particular the disk flares, so to get an exact solution one should take this flaring into account and iterate the process. However we have checked that the influence of the flaring is negligible.
2. since the solutions do not depend on the opacity coefficient contrary to the non irradiated case, **they are exact in the framework of the vertically averaged approximation**.

The optical thickness is smaller than unity beyond a radius of the order of 3 10^6 $R_{\rm S}$ for M_6=1, and 10^5 $R_{\rm S}$ for $M_6 = 100$ which is of the order of one parsec. When the disk is optically thin, the above solutions are not valid, since Eq. 21 is replaced by Eq. 22. For example one gets in the warping case:

$$T = 5.8\times10^2 (f_{-1}f_{\rm E})^{2/9} \frac{(1+\zeta)^{1/9}}{\zeta^{2/9}} R_4^{-1/9} \kappa_{\rm P}^{-2/9} \ {\rm K}. \quad (41)$$

As expected the temperature is almost constant with the radius.

3.2.2. Zero metallicity, optically thin disk

The solutions for the molecular region are given by Eqs. 15 to 17 and correspond to a flaring disk. Using the unperturbed scale height in the molecular regime given by Eq. 16, and equaling $F_{\rm inc}$ given by Eq. 32 to the viscous flux, one gets $R_{\rm crit}$:

$$R_{4,\rm crit} \sim 3\ \zeta^{0.101} (1+\zeta)^{.333} f_{\rm E}^{-0.101} f_{-1}^{0.77}, \quad (42)$$

which does not depend on the black hole mass.

Using then Eqs. 21, 22, 32, and A1, one finds the solution in the irradiation dominated region:

$$T = 800\ \zeta^{-0.303} (f_{-1}f_{\rm E})^{0.303} \ {\rm K}. \quad (43)$$

$$H = 3.6\times10^{12} f_{-1}^{-1} f_{\rm E}^{0.303} \times (1+\zeta)^{-1/2} \zeta^{-0.303} R_4^{3/2} M_6 \ {\rm cm} \quad (44)$$

$$\Sigma = 4.2\times10^4 \frac{\zeta^{0.697}}{(1+\zeta)} (f_{-1}f_{\rm E})^{0.303} \times M_6^{-1} R_4^{-3/2} {\rm g\ cm^{-2}}. \quad (45)$$

We see that the disk is flaring more than in the absence of irradiation, and the temperature is constant as expected. Again the disk stays cold and molecular.

If we assume backscattering of the central radiation, we find that the disk is dominated by irradiation at a small radius:

$$R_{4,\rm crit} = 0.07 f_{-1}^{-2}\ r_{\rm X,1}^{-1}. \quad (46)$$

For R larger than this radius, we get the corresponding pure irradiation solutions:

$$T = 2.6\times10^3 \left(\frac{\zeta^2}{1+\zeta}\right)^{-0.132} \times (f_{-1}f_{\rm E})^{0.263} r_{\rm X,1}^{0.132} R_4^{-0.263} \ {\rm K} \quad (47)$$

$$H = 6.3\times10^{12} \zeta^{-0.737} (1+\zeta)^{-0.132} \times (f_{-1}f_{\rm E})^{0.132} M_6 r_{\rm X,1}^{0.064} R_4^{1.37} \ {\rm cm}. \quad (48)$$

$$\Sigma = 10^5 \frac{\zeta^{0.263}}{(1+\zeta)^{0.132}} (f_{-1}f_{\rm E})^{0.132} M_6^{-1} R_4^{-1.63}. \quad (49)$$

In this case also the disk flares, and it would be necessary to combine the backscattering with the flaring to get the exact solution. However like in the previous case we have checked that the disk stays cold and molecular in the presence of this external radiation, and the structure is not dramatically modified.

The warping case is special. The disk structure is completely modified, as the critical radius is equal to $8 f_{-1} R_{\rm S}$. Actually the pure irradiation solution corresponds to a high temperature and to an optical thickness larger than unity up to a large radius, and our solutions are therefore not valid. Only a detailed computation including a correct determination of the opacity coefficient, which is out of the scope of this paper, would allow to determine the structure.

To illustrate this discussion, Fig. 5 shows the variation of the midplane temperature with the radius for the warped disk with a solar metallicity, and for the flaring disk with a zero metallicity. The solutions are actually valid only in a restricted range of radii. The upper limit of the radius is given by the requirement of a sufficiently large density and column density, and the lower limit in the zero metallicity case by the requirement of a molecular gas.

3.3. Penetration of the external radiative flux inside the disk

When a cold shell is illuminated by an ionizing flux of radiation, Lyman continuum photons are absorbed first, while X-rays penetrate more deeply inside. Since the absorption cross sections

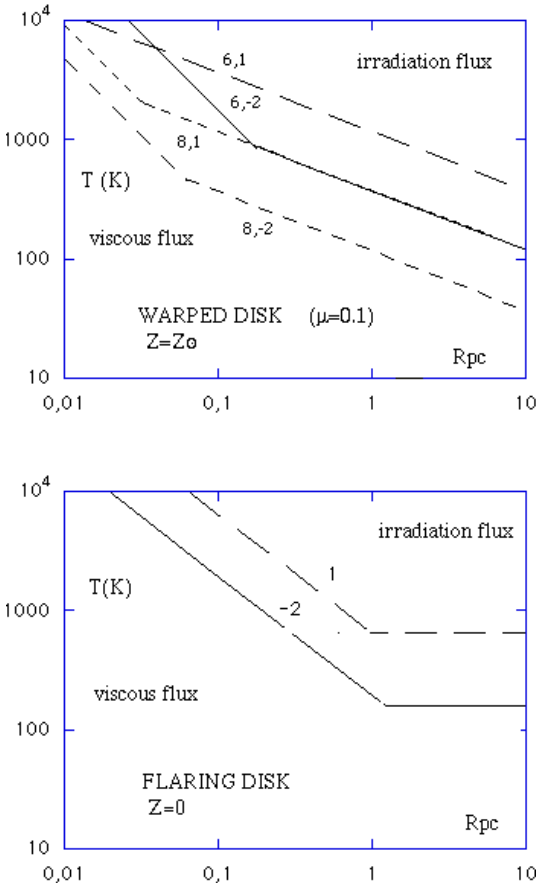

Fig. 5. T versus R in parsec for the warped disk with a solar metallicity, and for the flaring disk with a zero metallicity. The lines are labelled with the logarithm of the mass in $M_\odot$ and with the logarithm of the Eddington ratio $f_{\rm E}$. In the second case T does not depend on the mass.

decrease with energy, the heating and ionizing efficiency of the radiation decreases with depth, and so do the temperature and the ionization degree. The transition between the HII and the HI zone is abrupt, as in the Strömgren case, but the transition between the HI and the molecular zone is smoother. Nevertheless we shall schematize the vertical structure of the disk by 3 different zones: an upper ionized zone (HII), where the degree of ionization x (defined as $x = n_{\rm e}/n_{\rm HI}$) is larger than unity and the temperature is about 10^4 K, an intermediate atomic zone (HI), where x decreases and the temperature is equal to a few 10^3 K, and a molecular zone, where $x \leq 10^{-2}$ and the temperature is smaller than 2 10^3 K (see for instance Lepp et al. 1985 for the correspondance between the temperature and the ionization degree). Below a few Thomson depths, even hard X–rays and gamma rays are completely absorbed, and the gas is heated only by reprocessed visible and infrared radiation. In the case of a high radiation flux, a Compton heated corona at a temperature of a few 10^7 K can also be created above the disk, but in our case its column density is very small, and it does not absorb a sizable fraction of the flux, so it can be neglected.

To validate the results of the previous section, it is necessary to verify that the column density of the disk is much larger than the column densities of the ionized and of the atomic zones. The column density of the HII and the HI zones have been computed by Dumont and Collin-Souffrin (1990) in the case of an α-disk, and we shall repeat here this computation (with slight modifications) for the marginally unstable disk.

Since the disk is in hydrostatic equilibrium, the vertical variation of the pressure writes:

$$-\frac{1}{\rho}\frac{dP_{\rm g}}{dz} = \Omega^2(1+\zeta)z. \tag{50}$$

If the gas is isothermal at a temperature T, this equation integrates as:

$$n(z) = n_0 \exp\left(-\frac{z^2}{2H^2}\right), \tag{51}$$

where H is the scale height of the disk defined by Eq. A1 and n_0 is the midplane number density.

We can assume that the disk consists of two isothermal zones, the molecular zone at a temperature T_0 and the HI-HII zone at a temperature T_{1-2} (since the temperatures of the HI and HII zones are very close). The vertical structure can then be approximated by two gaussian profiles with two scale heights corresponding to these temperatures. Let us call H_0 and H_{1-2} the scale heights of the molecular and of the HI-HII zones, z_1, z_2 and z_3 the vertical coordinates of the limits of the central zone, of the HI zone and of the HII zone, $n_0(z)$, $n_1(z)$ and $n_2(z)$ the density in these zones, and $N_0(z)$, $N_1(z)$ and $N_2(z)$ the column densities. The scale heights satisfy the relation:

$$\frac{H_0}{\sqrt{T_0}} = \frac{H_{1-2}}{\sqrt{T_{1-2}}} \tag{52}$$

According to the continuity of pressure, the densities can be expressed as:

$$n_0(z) = n_0 \exp\left(-\frac{z^2}{2H_0^2}\right) \tag{53}$$

in the central zone, and

$$n_1(z) = n_2(z) = n_0 \frac{T_0}{T_{1-2}} \exp\left(-\frac{z_1^2}{2H_0^2}\right) \times \exp\left(-\frac{(z^2-z_1^2)}{2H_{1-2}^2}\right) \tag{54}$$

in the HI and in the HII zones.

Since the column density is dominated by the deepest layers, we can assume for simplicity that the density in each zone is given by $\langle n_2\rangle = n(z_2)$ and $\langle n_1\rangle = n(z_1)$. On the other hand if the column density of the disk is much larger than that of the HI and HII zones, we can identify N_0, $n_0(z=0)$, and H_0 with N (half the column density of the disk), n, and H respectively.

The column density of the HII zone is equal to:

$$N_2 = \int_{z_2} n_2(z)dz. \tag{55}$$

Using the approximation

$$\int_x \exp\left(-\frac{t^2}{2}\right)dt \sim \frac{\exp\left(-\frac{x^2}{2}\right)}{x}, \tag{56}$$

Eq. 55 becomes:

$$N_2 \sim N \frac{H}{z_2} \frac{1}{\sqrt{\pi}} \exp\left(-\frac{z_2^2}{2H^2}\right). \quad (57)$$

where N is equal to $\sqrt{(\pi/2)}(\Sigma/m_{\rm H})$.

The same expression can be used for the column density of the HI zone, simply replacing z_1 by z_2, provided that $z_1^2 \ll z_2^2$.

3.3.1. The HII zone

In this zone, ionization is dominated by Lyman continuum photons, so one can simply assume that all the ionizing photons are absorbed in the HII zone. One gets then the column density of the HII shell:

$$N_2 = \frac{F_{\rm inc} m_{\rm H}}{\langle h\nu \rangle_{\rm ion} \langle n_2 \rangle \alpha(T)}, \quad (58)$$

where $\langle h\nu \rangle_{\rm ion}$ is the mean energy of ionizing photons, about equal to 1 Rydberg, $\alpha(T)$ is the hydrogen recombination coefficient, of the order of $5\,10^{-13}$ cm^3 s^{-1} for the typical temperature of an HII region.

Using the solutions for Σ found in the previous section for the irradiation cases, Eqs. 5, 30, 31 32, 51, 57 and 58, one gets the solutions for z_2, and for N_2/N.

Eqs. 30, 31 and 32, show that among all possibilities for external irradiation, warping is the most efficient. In the solar metallicity case, we shall compute the column densities of the different zones in this case to get an overestimation of the influence of the external flux. In the zero metallicity case, we shall simply take into account the flaring of the disk. It is clear that such computations can be easily repeated for any external radiative flux. One gets:

– for the warped disk with the solar metallicity:

$$\frac{N_2}{N} \sim 10^{-5} \sqrt{\frac{H}{z_2}} \sqrt{\frac{T_{1-2}}{T}} \frac{(1+\zeta)^{1/4}}{\zeta} \times (f_{-1} f_{\rm E})^{7/16} M_6^{17/16} R_4^{21/16}, \quad (59)$$

– for the flaring disk with zero metallicity:

$$\frac{N_2}{N} \sim 2 \times 10^{-7} \sqrt{\frac{H}{z_2}} \sqrt{\frac{T_{1-2}}{T}} \zeta^{-1}\, M_6\, R_4^{3/2}, \quad (60)$$

where $\sqrt{H/z_2}\sqrt{T_{1-2}/T}$ is of the order of unity.

As required N_2 is much smaller than the column density of the disk itself, except for large black hole masses and large values of R_4, corresponding to a large radius. Up to a radius of one parsec, the condition is fulfilled and our approximations are valid.

3.3.2. The HI zone

After the Lyman continuum has been absorbed in the HII zone, ionization is provided by X–ray photons. Each photoionizations give rise to many subsequent ionizations by secondary electrons. As shown by Bergeron and Collin-Souffrin (1971), a primary photon of energy $h\nu$ gives a the mean number of secondary ionizations of about $h\nu/(30{\rm eV})$. Let us assume that the incident continuum is a power law with an index equal to unity. The rate of ionization per hydrogen atom is then:

$$\xi \sim 10^{-1} \frac{F_{\rm inc}}{30\,{\rm eV}} \int_{h\nu_{\rm min}} \sigma(\nu) \frac{d\nu}{\nu} \qquad {\rm s}^{-1}, \quad (61)$$

where $\sigma(\nu)$ is the photoionization cross section and $h\nu_{\rm min}$ is defined by:

$$N_1 \sigma(\nu_{\rm min}) = 1. \quad (62)$$

Equaling the rate of ionization to the rate of recombination, one gets the relation between ξ and the degree of ionization:

$$\xi = 10^{-4} \alpha(T)\ \langle n_1 \rangle\, x_{-2}^2, \quad (63)$$

where x_{-2} is the degree of ionization in 10^{-2}, and $\alpha(T)$ is now about equal to 10^{-12} cm^3 s^{-1} for the temperature of the HI zone.

Approximating $\sigma(\nu)$ by the hydrogen cross section $\sigma(\nu_{\rm Lyman}) \times (\nu/\nu_{\rm Lyman})^{-3}$, and proceeding as before, one gets:

– for the warped disk with the solar metallicity:

$$\frac{N_1}{N} \sim 10^{-4} \sqrt{\frac{H}{z_2}} \sqrt{\frac{T_{1-2}}{T}} \frac{(1+\zeta)^{1/4}}{\zeta} \times (f_{-1} f_{\rm E})^{7/16} x_{-2}^{-1} M_6^{17/16} R_4^{21/16}, \quad (64)$$

– for the flaring disk with zero metallicity:

$$\frac{N_1}{N} \sim 2 \times 10^{-6} \sqrt{\frac{H}{z_2}} \sqrt{\frac{T_{1-2}}{T}} \zeta^{-1}\, x_{-2}^{-1}\, M_6\, R_4^{3/2}. \quad (65)$$

So again the column density of the HI zone is much smaller than that of the disk up to about one parsec and the disk is predominantly molecular. However one should keep in mind that below the HI zone, there is an "excited molecular zone", where non absorbed hard X–rays might contribute slightly to the ionization and to the heating of the gas.

In summary we have seen that at a distance from the center between 0.01 and 1 parsec, the external radiative flux can maintain only a thin layer near the surface of the disk in an atomic or ionized state (note that **the thickness of the HII and HI zones does not depend on the abundances**, although the mean optical thickness is very different in the zero and in the solar metallicity cases; this is due to the fact that hydrogen atoms alone determine this thickness). However the midplane temperature is higher than in the pure viscous case, and the scale height is increased accordingly, but the whole radial profile is not dramatically modified, except if the disk is warped. We should also remember that the influence of the incident flux has been overestimated in all these computations (for instance we have neglected a possible limb darkening effect of the central source).

3.4. Application to NGC 4258

NGC 4258 constitutes an ideal object for applying these results. Since the discovery of intense water maser spots in Keplerian

motion in this galaxy (Miyoshi M. et al. 1995), it is believed that NGC 4258 harbors a massive black hole, whose mass is estimated to be 3 $10^7 \mathrm{M}_\odot$. The 2-10 KeV X-ray luminosity is equal to 4 10^{40} ergs s^{-1}, corresponding to an Eddington ratio f_E of the order of 10^{-5}, and to an accretion rate $\sim 10^{-5}\mathrm{M}_\odot\,\mathrm{y}^{-1}$. However Lasota et al. (1996) have proposed that the gas inflow in the inner part of the disk is advection dominated, meaning that the mass efficiency conversion factor is much smaller than the standard value of 0.1, and that the accretion rate is consequently much higher ($\sim 10^{-2}\mathrm{M}_\odot\,\mathrm{y}^{-1}$).

An important question is whether the masing region can be identified with an accretion disk, as proposed by Neufeld, Maloney & Conger (1994) and Neufeld and Maloney (1995). The masing spots are located between 0.13 and 0.25 pc. They display a strong warping, reaching an angle of 25° at 0.25 pc. So the accretion disk would be illuminated by the X–ray source, and the maser could be a natural consequence of this irradiation.

Huré & Collin (1998) have shown that the disk at the radius of the maser spots is self-gravitating in the framework of an α-disk, and that the thickness of the disk is much larger than the scale height of the spots, and that the density is much larger than that required by the maser. Another conclusion was that the irradiation does not modify the structure of the disk. However these results were obtained for an α-disk, while the masing region is located beyond the Toomre radius. So it is interesting to perform the computation using the marginal instability prescription, which corresponds to a much lower density than the α-disk. In particular according to Eq. 5 the midplane density is now of the order of $10^{10}\,\mathrm{cm}^{-3}$ at a radius of 0.2 pc, while it was of the order of $10^{13}\,\mathrm{cm}^{-3}$ in the case of the self-gravitating α-disk.

The critical radius beyond which the irradiation dominates is given by Eq. 34 with f_{-1} replaced by the cosinus of the warping angle, μ_{-1} (in units of 0.1). Here it is necessary to introduce the efficiency conversion factor η_{-1} (in units of 0.1, the value used in the present paper), to take into account the possibility of an advection dominated disk. One gets then for $M = 310^7\mathrm{M}_\odot$:

$$R_\mathrm{crit} \sim 10^{-1}\eta_{-1}^{-1/3}\frac{\zeta^{8/21}}{(1+\zeta)^{4/21}}\mu^{-6/21}f_\mathrm{E}^{1/21}\kappa_\mathrm{R}^{8/21}\ \mathrm{pc}. \qquad (66)$$

It is interesting that R_crit almost does not depend on the Eddington ratio, but depends on the efficiency factor. In the case of a standard efficiency, the masing region is dominated by the irradiation flux, while it is dominated by the viscous flux if the efficiency is smaller. So the two cases lead to different results concerning the midplane temperature, the scale height, and the optical thickness. A detailed study involving the computation of the vertical structure is in progress to check whether the conditions in the disk are appropriate for the maser emission (Sincell & Collin 1998).

4. Conclusion

Within the framework of vertically averaged stationary disk model, we have shown that pure H-He disks and disks with a solar metallicity have very different properties, especially for small black hole masses. In particular pure H-He disks flares, so the masses of the fragments which can form due to the gravitational instability increase with the radius in the zero metallicity case, while they decrease in the solar metallicity case. This result has important consequences on the star formation and evolution in primeval disks.

We have also shown that, contrary to a widespread idea, irradiation by a central X–ray source does not affect dramatically the disk structure, which stays molecular up to large distances. Only a thin layer near the surface is in an atomic or in an ionized state. This result is a consequence of the marginal instability prescription. Indeed the midplane density, whatever the heating flux (viscous or radiative), is proportional to R^{-3}, while in an α-disk, the equations of the structure are highly non linear, and any change of the heating flux has strong repercussions on the density and consequently on the temperature and on the scale height. Actually the marginal instability prescription leads to a **universal structure which depends very little on the details of the model**. Note also that all conclusions are almost independent of the Eddington ratio, since the density does not depend on the accretion rate, contrary to the case of α-disks. However the critical radius beyond which the external irradiation flux dominates on the viscous flux depends on the mass energy efficiency factor.

We have found analytical solutions for the optically thin case (primeval disks) and for the optically thick one (solar metallicity), taking into account the irradiation. They can be used in a first approximation to determine the radial profile in the marginally unstable region. In the irradiation dominated case with solar metallicity these solutions do not depend on the opacity, and are therefore exact in the framework of the vertically averaged model. However they are not valid when the column density is smaller than about one Thomson depth, as hard X–ray photons can then penetrate down to the midplane, and excite the gas.

As an application, we have shown that the masing spots in the NGC 4258 are located in the viscously dominated region for a large accretion rate, and in the irradiation dominated region for a low accretion rate. The analytical solutions given here are also used in a following paper to study star formation and star evolution inside accretion disks (Collin & Zahn, 1998).

We stress that a weakness of our work lies in the grey approximation (mean opacities) used to compute the structure of the optically thin regime. This is particularly important in the irradiation dominated disk when the surface density is smaller than $1\,\mathrm{g\,cm}^{-2}$, since hard X-rays can penetrate down to the midplane and modify the emissivity of the molecular gas. On the contrary, in the solar case even if the density is low, the opacity due to grains should remain of the order of $1\,\mathrm{cm}^2\,\mathrm{g}^{-1}$. We recall also that this work does allow only to determine the scale height, the surface density, and the averaged (i.e. midplane) values of the temperature and of the density as functions of the radius. Any study aiming for instance at determining the spectrum emitted by the disk requires a more detailed computation taking into account the vertical structure.

Acknowledgements. We gratefully thank J.P. Lasota, G. des Forêts and E. Roueff for fruitful discussions, M. Sincell for having pointed an error in the computations, and J. Silk for pointing the role of HD in the cooling.

Appendix A: equations of the disk structure in the gravitationally stable region

The radial structure of a stationary geometrically thin vertically averaged accretion disk (Shakura & Sunyaev 1973; Pringle 1991; Frank et al. 1992 for a review), including self-gravitation, is computed on the basis of the following equations:

– the equation of hydrostatic equilibrium:

$$\frac{P}{\rho H} = \Omega^2 H\,(1+\zeta)\,, \tag{A1}$$

where H is the scale height, ρ is the density, Ω is the Keplerian angular velocity, $\zeta = 4\pi G\rho/\Omega^2$ is the correction for self-gravity, and P is the sum of the gas pressure:

$$P_{\rm g} = \frac{\rho k T}{\mu m_{\rm H}}, \tag{A2}$$

where T is the midplane temperature, μ is the mean mass per particle, and of the radiative pressure:

$$P_{\rm rad} = \frac{F_{\rm rad}}{c}\left[\frac{1}{2}\tau_{\rm R} + \frac{1}{\sqrt{3}}\right]. \tag{A3}$$

$\tau_{\rm R}$ is the Rosseland optical depth, and $F_{\rm rad}$ is the flux radiated by each face of the disk (Hubeny 1990):

$$F_{\rm rad} = \frac{4}{3}\frac{\sigma T^4}{\frac{1}{2}\tau_{\rm R} + \frac{1}{\sqrt{3}} + \frac{1}{3\tau_{\rm P}}}, \tag{A4}$$

where $\tau_{\rm P}$ is the Planck optical depth. Note that, in the optically thick case, $P_{\rm rad}$ tends to its LTE value and $F_{\rm rad} \approx \sigma T^4/\tau_{\rm R}$, while in the optically thin case, the radiative pressure begins negligeable with respect to the gas pressure and $F_{\rm rad} \approx \tau_{\rm P}\sigma T^4$.

– the energy balance between the local viscous dissipation and the radiative cooling:

$$F_{\rm rad} = \frac{3\Omega^2 \dot{M}}{8\pi} f(R), \tag{A5}$$

where $\dot{M}$ is the mass accretion rate, and $f(R)$ accounts for the inner boundary conditions (for outer regions, we can take $f(R) = 1$).

– the α-prescription which defines a phenomenological viscosity coefficient:

$$\nu = \alpha\sqrt{\frac{P}{\rho}}H, \tag{A6}$$

α being dimensionless, and ν being the kinematic viscosity.

– the equation accounting for the transport of angular momentum:

$$\frac{\dot{M} f(R)}{3\,\pi} = 2\nu\rho H \tag{A7}$$

These equations, when solved self-consistently with the appropriate functions for $\kappa_{\rm R}(\rho,T)$, $\kappa_{\rm P}(\rho,T)$ and $\mu_{\rm P}(\rho,T)$, yield the disk structure for $R \leq R_{\rm T}$ (see Sect. 2 for the definition of the Toomre radius $R_{\rm T}$).

Finally, an approximation has been made to simplify the computations, both analytically and numerically. In the optically thick case, we have taken:

$$F_{\rm rad} = \frac{8\sigma T^4}{3\kappa_{\rm R}\rho H}. \tag{A8}$$

Actually, Eqs. (A1)-(A3) and (A5)-(A7) can be combined into the following unique equation, without any assumption on the pressure and on ζ:

$$\dot{M}^{3/2} - \left(\frac{3\alpha}{2G}\right)\frac{P^{3/2}}{\rho^{3/2}}\dot{M}^{1/2} + \left(\frac{16\sigma\sqrt{6\pi\alpha}}{9G}\right)\frac{P^{1/4}T^4}{\kappa_{\rm R}\rho^{7/4}} = 0 \tag{A9}$$

which can be easily solved, given the accretion rate, inside the (ρ,T)-plane using the method described in Huré (1998). Since no optically thin solution does exist for an α-disc, we will not give here a similar expression corresponding to the optically thin regime.

Appendix B: equations of the disk structure in the gravitationally unstable region

To compute the disk structure beyond the Toomre radius ($R \geq R_{\rm T}$), all the above equations hold, except that Eq. (A7) is replaced by the prescription for marginal stability:

$$Q = cste \sim 1 \tag{B1}$$

which corresponds to $\zeta \sim 4$ in Eq(A1). Note that a value of α in the gravitationally unstable region can then be inferred using Eq. (A6), but it does not have any physical meaning (Collin & Zahn, 1998).

As for the α-prescription, the equation set including now Eq. (B1) can be reduced to a unique expression. For the optically thick part of the disc at marginal instability, this expression is:

$$\dot{M}^2 - \left(\frac{2^{10}\,\pi\sigma^2}{3^4\,G\kappa_{\rm R}^2}\right)\frac{T^8}{P\rho^2}\zeta(1+\zeta) = 0 \tag{B2}$$

with $\zeta =$. For the optically thin part of the disc, we have:

$$\dot{M}^2 - \left(\frac{16\,\sigma^2\kappa_{\rm P}^2}{9\,\pi G^3}\right)\frac{PT^8}{\rho^2}\frac{\zeta^3}{1+\zeta} = 0 \tag{B3}$$

also with a fixed value for ζ. The solutions of both Eqs. (B2) and (B3) are computed like the solution of Eq. (A9).

References

Alexander D.R., Ferguson J.W., 1994, ApJ 437, 879
Bergeron J., Collin-Souffrin S., 1971, A&A 11, 40
Pollack J.B., Hollenbach D., Beckwith S., et al., 1994, ApJ 421, 615
Cannizzo J.K., 1992, ApJ 385, 94

Cannizzo J.K., Reiff C.M., 1992, ApJ 385, 87
Collin-Souffrin S., Dumont A.M., 1990, A&A 229, 292
Collin S., Zahn, J-P., 1998, in preparation
Dumont A.M, Collin-Souffrin S., 1990, A&A 229, 302
Goldreich P., Linden-Bell D., 1965, MNRAS 130, 97
Frank J., King A., Raine D., 1992, Accretion power in astrophysics. 2nd Ed., Cambridge University Press
Hubeny I., 1991, In: Bertout C., Collin-Souffrin S., Lasota J.-P., Tran Thanh Van J. (eds.) Structure and emission properties of accretion disks. Eds Frontières, p. 227
Huré J.M., 1994, thesis, University Paris 7
Huré J.M., Collin-Souffrin S., Le Bourlot J., Pineau des Forets G., 1994a, A&A 290, 34
Huré J.M., Collin-Souffrin S., Le Bourlot J., Pineau des Forets G., 1994b, A&A 290, 19
Huré J.M., 1998, A&A, in press
Huré J.M, Collin S., 1998, to appear in: Holdt S. (ed.) Proceedings of the 8th Maryland Conference, Accretion processes in astrophysical systems. AIP press
Lasota J.P., Abramowicz M.A., Chen X., et al., 1996, 1pJ 462, 142
Lepp S., Shull J.M., 1983, ApJ 270, 578
Lepp S., McCray R., Shull J.M., Woods D.T., Kallman T., 1985, ApJ 288, 58
Lin D.N.C., Pringle J.E., 1987, MNRAS 225, 607
Loeb A., Rasio F.A., 1994, ApJ 432, 52
Malkan M.A., Sargent W.L.W., 1982, ApJ 254, 22
Miyoshi M., et al., 1995, Nat 373, 127
Neufeld D.A., Maloney P.R., Conger S., 1994, ApJL 436, L127
Neufeld D.A., Maloney P.R., 1995, ApJL 447, L17
Paczynski B., 1978, AcA 28, 91
Puy D., 1997, New Astronomy 2, 299
Shakura N.I., Sunyaev R.A., 1973, A&A 24, 337
Shlosman I., Frank J., Begelman M.C., 1989, Nat 338, 45
Siemiginowska A., Czerny B., Kostyunin V., 1996, ApJ 458, 491
Sincell M., Collin S., 1998, submitted to A & A
Smith M.D., Mac Low M.M, 1997, A&A 326, 801
Tiné S., Lepp S., Gredel R., Dalgarno A., 1997, ApJ 481, 282
Toomre A., 1964, ApJ 139, 1217